Mössbauer Effect Reference and Data Journal

April 2013 • Volume 36 • Number 4

CHEMICAL APPLICATIONS

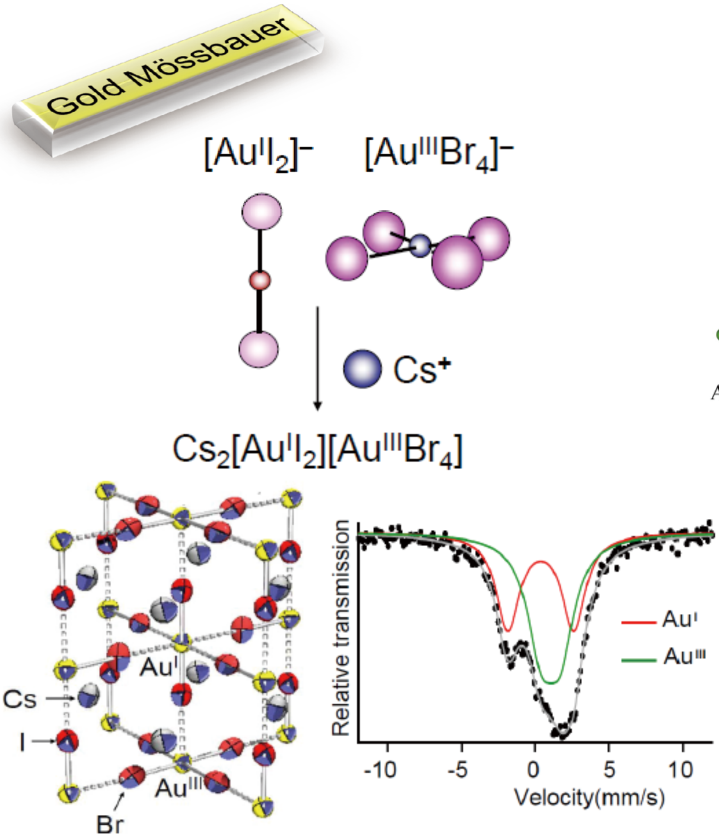

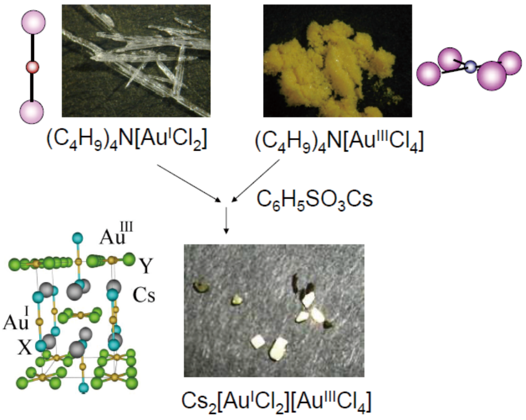

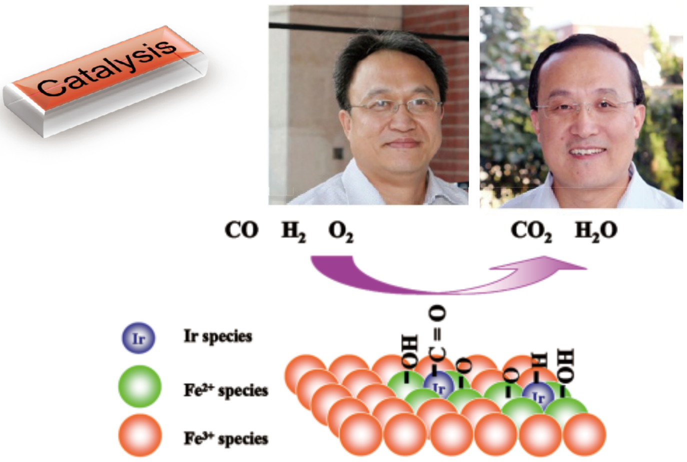

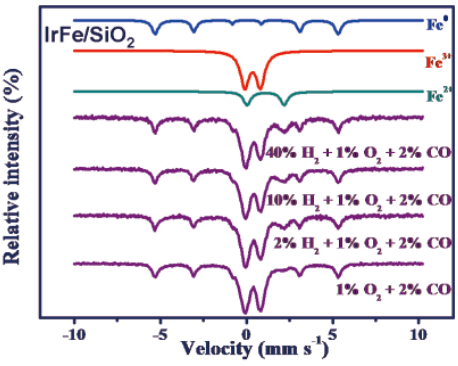

Quasi in situ ^{57}Fe Mössbauer spectroscopic study for PROX over IrFe catalyst

Kuo Liu,[a] Junhu Wang (✉), Tao Zhang (✉)
Dalian Institute of Chemical Physics, Chinese Academy of Sciences, 457 Zhongshan Road, Dalian, 116023, China.
[a] Present address: Research Center for Eco-Environmental Sciences, Chinese Academy of Sciences, Beijing, 100085, China.
Email: taozhang@dicp.ac.cn (T. Zhang), wangjh@dicp.ac.cn (J. Wang)

Abstract

By using quasi in situ Mössbauer spectroscopy, the positive effect of iron oxide in the IrFe bimetallic catalysts was investigated for preferential CO oxidation in H_2-rich conditions (PROX). Quasi in situ Mössbauer spectroscopic studies gave a clear picture for the distribution of different iron species under different reaction conditions, and determine different iron species both quantitatively and qualitatively, providing important information for a deeper insight into the mechanism of the PROX reaction over the bimetallic catalysts. The results of the Mössbauer studies showed that the amounts of Fe^{2+} species in the $IrFe/SiO_2$ bimetallic catalysts increased with the increase of H_2 fraction in the PROX gas mixtures, and this trend was consistent with that of the CO oxidation rate. For the $IrFe/Al_2O_3$ bimetallic catalysts, the impregnation sequences during the catalyst preparation process influenced the amounts of the active Fe^{2+} species and the CO oxidation rate increased with the amounts of the active Fe^{2+} species. Both the Mössbauer results on the $IrFe/SiO_2$ and $IrFe/Al_2O_3$ bimetallic catalysts strongly suggested that the Fe^{2+} is the active site for oxygen activation during the PROX reaction.

Kuo Liu

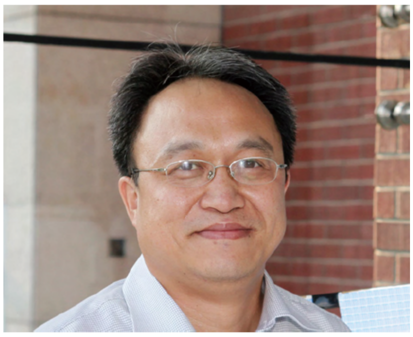

Junhu Wang

Tao Zhang

Kuo Liu received her doctorate degree in Industrial Catalysis at Dalian Institute of Chemical Physics. She successfully finished her diploma work in the State Key Laboratory of Catalysis supervised by Prof. Tao Zhang and Prof. Jianyi Shen from Nanjing University. Her PhD thesis focused on the topic: Mechanistic Studies (Mössbauer and kinetic study) on Preferential Oxidation of CO in H_2-rich Atmosphere (PROX) over IrFe Catalysts. She is now a postdoctoral fellow at Research Center for Eco-Environmental Sciences, Chinese Academy of Sciences, working on the mechanistic study of the selective catalytic reduction of NO_x with NH_3 (NH_3-SCR) over metal oxide catalysts.

Junhu Wang got his doctorate degree at Toho University in Japan in 2002. He became a Professor in 2008 at Dalian Institute of Chemical Physics, Chinese Academy of Sciences, and he has been granted the outstanding scholarship foundation of CAS (100 Talents Program) for the applications of in-situ Mössbauer technique in China. He started his Mössbauer study since 1996. His doctoral thesis focused on Mössbauer spectroscopic studies on gadolinium, erbium and neptunium compounds. He has more than 30 published papers and one chapter of book related with Mossbauer studies. His main research area at present includes "development and application of novel catalytic materials" and "in-situ Mössbauer characterization".

Tao Zhang got his doctorate degree at Dalian Institute of Chemical Physics, Chinese Academy of Sciences in 1989. He became a Professor in 1995, and he is now the Director of Dalian Institute of Chemical Physics. He started his Mössbauer study from 1980s. His doctoral dissertation title was "study of carbon deposition on highly dispersed Pt/Al_2O_3 and Pt-Sn/Al_2O_3 catalysts for dehydrogenation of alkanes. He has ever studied in Prof. Frank Berry's group at the University of Birmingham for one year. His main research area is industrial catalysis at present, including "catalytic decomposition technology for non-toxic propellants", "new catalytic materials", and "environmental catalysts".

Introduction

Preferential CO oxidation in H_2-rich conditions (PROX) is an effective way to remove CO in the H_2 fuel for polymeric electrolyte membrane fuel cells (PEMFCs). During the past decade, various catalysts for the PROX reaction have been investigated in a wide operational temperature ranged from 80 to 180 °C, and noble metals promoted by a reducible metal oxide are considered as the best candidates [1-3]. For example, Pt-based catalysts promoted by CeO_x [4], TiO_x [5], SnO_x [6], and FeO_x [7-10] were reported to be highly effective for the PROX reaction, especially at lower temperatures (< 80 °C). These catalysts followed a non-competitive bifunctional catalytic mechanism, in which CO adsorbed on the Pt-based noble metal site reacts with oxygen activated on the reducible metal oxide at the interface of noble metal and the oxide [10,11]. Although it has been widely accepted that the metal oxide played an important role of activating O_2, it is still controversial what the oxidation states of the reducible metal is under the reaction conditions. Sirijaruphan et al. [12] indicated that the re-oxidation of Fe during the reaction is likely a significant reason for the loss of activity of the PtFe catalyst. Kotobuki et al. [13] studied the state of Fe in PtFe/mordenite catalyst by X-ray absorption near edge structure (XANES), and they claimed that the Fe mainly existed as FeO after H_2 pretreatment. Sun et al. [14] proposed that CO oxidation proceeded through the formation of an oxygen-rich FeO_x ($1 < x < 2$) film that reacted with CO on the FeO(111)/Pt(111) film by employment of scanning tunnel microscope (STM), low energy electron diffraction (LEED), auger electron spectroscopy (AES) and temperature programmed desorption (TPD). Bao's group pointed out Fe^{2+} played an important role by combining surface science studies and theoretical methods [15]. However, these studies were mostly qualitative and did not give a clear picture for the distribution of different Fe species on the catalyst surface.

The effect of H_2 is also important in the PROX reaction, and the importance of H_2 was reported for gold-based catalysts in the previous literatures [16-19]. However, the systematic study of the H_2 effect on the PROX reaction over MO_x-promoted noble metal catalysts was still lacking [20,21]. It is widely accepted that the presence of H_2 could promote the activity of CO oxidation at low temperatures, but inhibit CO oxidation at high temperatures owing to the competition reactions. Many literatures reported the promotional mechanism of H_2 at low temperatures. Some authors proposed that H_2 adsorbed on Pt spilt on the support surface, forming hydroxyl groups or adsorbed water that could contribute directly to the CO conversion via low-temperature water-gas shift reaction [4,22]. On the other hand, some investigations pointed out that the adsorbed water enhanced the CO oxidation mainly by promoting the decomposition of carbonate or formate [23,24]. However, none of the above authors have taken into consideration the correlation between H_2 concentration and the oxidation states of M in the MO_x.

Mössbauer spectroscopy is a powerful tool to identify the oxidation states of iron [25-30], and the relative amounts of different Fe species can be quantitatively determined [31]. Aiming to characterize many kinds of novel iron-bearing energy and environmental catalytic materials under their working conditions, our group developed a specially designed quartz reactor for quasi in situ ^{57}Fe Mössbauer measurement, which was similar to that described in Ref. 32, as shown in Figure 1. The catalyst in the quartz reactor was treated by different gas mixtures. After cooling to room temperature in He flow, both stopcocks were closed to seal the reactor filled with He gas. Then, the sample was moved into the side cell, and a Mössbauer spectrum of the sample was measured at room temperature. The ^{57}Fe Mössbauer spectra were recorded on a Topologic 500A spectrometer and a proportional counter at room temperature. ^{57}Co(Rh) moving in a constant acceleration mode was used as radioactive source. All of the spectral analyses were conducted assuming a Lorentzian line shape for computer folding and fitting. The Doppler velocity of the spectrometer was calibrated with respect to α-Fe foil. And the free recoil fraction was assumed to be the same for all iron species. Mössbauer parameters such as the isomer shift (IS), the electric quadrupole splitting (QS), the full line width at half maximum (FWHM), the magnetic hyperfine field (MF), and the relative resonance areas of the different components of the absorption patterns (RI) were determined. In this way, we achieved quasi in situ studies of ^{57}Fe Mössbauer measurement, and gave a clear picture for the distribution of different Fe species on the catalyst surface and bulk under the reaction conditions.

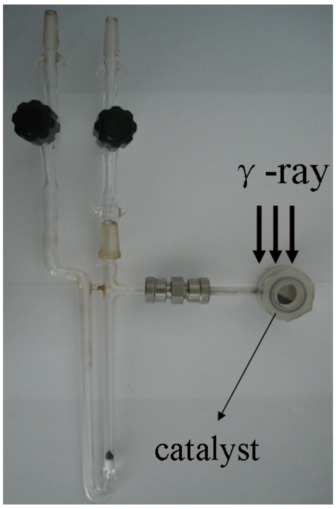

Figure 1. Reactor for quasi in situ Mössbauer characterization.

In our previous Mössbauer studies, we chose the IrFe catalysts as the subject investigated due to their significantly enhanced performances in the PROX reaction in comparison with non-promoted Ir catalyst [33-35]. Both the effect of H_2 fractions and the impregnation sequences during the preparation process on the catalytic behavior of the IrFe catalysts were studied in detail by quaisi in situ Mössbauer spectroscopy [36,37]. In the present review, the influence of H_2 concentration on the oxidation state of Fe species and the CO oxidation rate in our IrFe catalyst has been presented in the first part, while the influence of the impregnation order on the Fe oxidation state and the CO oxidation rate has been presented in the second part. In both parts, a quantitative analysis of different Fe species after being subjected to treatments with various feed gas mixtures by quasi in situ ^{57}Fe Mössbauer spectroscopy has been given in detail. ^{57}Fe Mössbauer spectroscopic results provided strong evidence that Fe^{2+} species in the IrFe catalysts is responsible for activating oxygen in the PROX reaction.

2. PROX reaction over IrFe/SiO_2

2.1 Catalytic activities - the effect of H_2

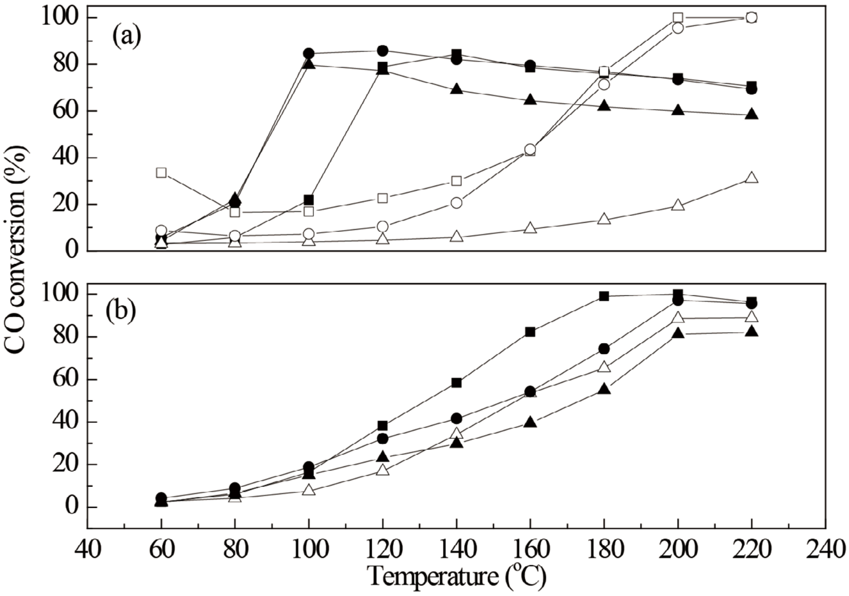

Figure 2. CO conversions vs. temperature over IrFe/SiO_2 (a) and Ir/SiO_2 (b). The reaction feed gas contains various volume fractions of H_2: (Δ) 0 %, (■) 2 %, (●) 10 %, and (▲) 40 %, or the fractions of H_2O: (□) 10 %, (○) 2 %; GHSV = 40,000 mL h^{-1} g_{Cat}^{-1}.

The results of the systematic study by varying the H_2 concentration ranging from 0 to 40 % in the feed gas have been shown in Figure 2. The figure illustrates CO conversions with the reaction temperature under different feed gas compositions over the IrFe/SiO_2 and Ir/SiO_2 catalysts. For IrFe/SiO_2 (Figure 2a), the activity of CO oxidation was low in the absence of H_2. CO conversion was lower than 40 % even when the temperature was 220 °C. However, CO conversion was increased significantly when 2 % H_2 was added, and the highest CO conversion was 85 % at 140 °C. When H_2 concentration was increased from 2 % to 10 %, the temperature for the maximum CO conversion was shifted to 120 °C. If H_2 concentration was further increased to 40 %, the CO conversions below 100 °C were the same as those in the case of 10 % H_2, whereas the CO conversions above 100 °C decreased significantly due to the competition between H_2 and CO oxidation, which became more pronounced either when H_2 concentration or the reaction temperature was increased [16]. The activity results of the PROX reaction on the IrFe/SiO_2 catalyst demonstrated that the presence of H_2 promoted the CO oxidation significantly at low temperatures, and the promotional effect was closely related to the H_2 fractions in the feed gas. The results on the IrFe catalysts below 100 °C were in agreement with Pt/Al_2O_3 catalyst reported by Kim and Lim [21]. However, they did not consider the effect of H_2 at lower H_2 concentrations.

The addition of H_2O was also reported to promote the low-temperature CO oxidation [4,22], therefore, the effect of water vapor on CO oxidation over the IrFe catalysts was also investigated. As shown in Figure 2a, CO conversion was indeed enhanced either when 2 % or 10 % H_2O was present in the feed gas. However, compared with the effect of H_2, the promotional effect of H_2O on CO oxidation was far less pronounced when the temperature was lower than 160 °C. The results may indicated that H_2 and water promoted CO oxidation in different ways. CO conversion was increased greatly by adding water only when the temperature was higher than 160 °C, thus, water gas shift reaction may contributed to CO oxidation significantly at such high temperatures [38].

As shown in Figure 2b, the promotional effect of H_2 on CO oxidation was also observed for Ir/SiO_2 catalyst. However, compared with IrFe/SiO_2, this effect was much less remarkable, especially at lower temperatures (< 140 °C). When comparing Figure 2a and 2b, it could be seen that Ir/SiO_2 catalyst was even more active than IrFe/SiO_2 catalyst in the absence of H_2. Therefore, it could be deduced that Fe did not have any positive effect for CO oxidation in the absence of H_2. In addition, the acceleration of CO oxidation became smaller owing to the competition of H_2 and CO oxidation with the increase in H_2 concentration on Ir/SiO_2, and this trend was different from the case of IrFe/SiO_2. This result showed that the promotional effect of Fe is closely related to the presence of H_2. H_2 concentration in the feed gas influenced greatly the distribution of different Fe species in the IrFe catalyst.

2.2 The activation of O_2 - Microcalorimetric study

Microcalorimetric study has been conducted on both IrFe/SiO_2 and Ir/SiO_2 to reveal the adsorption behaviors of reactant molecules (CO, O_2, and H_2). As shown in Figure 3 and Table 1, the adsorption of CO was much stronger than H_2 on the Ir/SiO_2 catalyst, and both the adsorption of H_2 and CO was weakened greatly on the IrFe/SiO_2 catalyst in comparison with Ir/SiO_2. According to the initial adsorption heat value of H_2, it can be inferred that H_2 can not be chemically adsorbed on the IrFe/SiO_2 catalyst. The saturation uptake of CO was only 20 μmol g_{Cat}^{-1}, which was significantly decreased by about 80 % in comparison with that on Ir/SiO_2, indicating that Fe species could decrease the adsorption amount and strength of CO on the IrFe catalysts. This result is similar to that was reported on the PtFe catalyst [9]. In addition, as reported previously, in situ diffuse reflectance infrared spectroscopy (DRIFTS) study for CO adsorption on the Ir/SiO_2 and IrFe/SiO_2 catalysts confirmed again that the addition of Fe weakened CO adsorption greatly [36], indicating that Fe species blocked most of the Ir metal surface [39], which was in good agreement with the microcalorimetric results. On the contrary, the saturation uptake of O_2 adsorption on the IrFe/SiO_2 catalyst was significantly increased, from 55 μmol g_{Cat}^{-1} on Ir/SiO_2 to 240 μmol g_{Cat}^{-1} on IrFe/SiO_2, indicating that the addition of Fe species facilitated O_2 adsorption on the IrFe catalyst. This result was consistent with that obtained by chemisorption reported in the literature [35]. It is widely accepted that CO oxidation on an unpromoted noble metal catalyst follows a competitive Langmuir-Hinshelwood mechanism where CO, H_2, and O_2 are all adsorbed on the noble metal surface. In the case of the Ir/SiO_2 catalyst, the stronger adsorption of CO than H_2 (Table 1) would be favorable to the preferential oxidation of CO even under the presence of rich H_2 atmosphere. At the same time, however, the strong adsorption of CO makes the Ir sites almost fully covered by CO at low temperatures which leads to only a few sites available for oxygen adsorption [1]. In such a case, the CO conversions on the Ir/SiO_2 catalyst at low temperatures are very low, as shown in Figure 2b. To enhance the activity for low temperature CO oxidation on the Ir monometallic catalyst, the adsorption of CO on the Ir sites must be weakened so that O_2 has enough opportunities to adsorb on them. For this purpose, the second metal Fe is added. Microcalorimetry has shown that the addition of Fe indeed weakens the adsorption of CO greatly. In this case, the possibility for the reaction between adsorbed CO and O on the neighboring Ir sites, i.e., competitive Langmuir-Hinshelwood reaction, should have been enhanced.

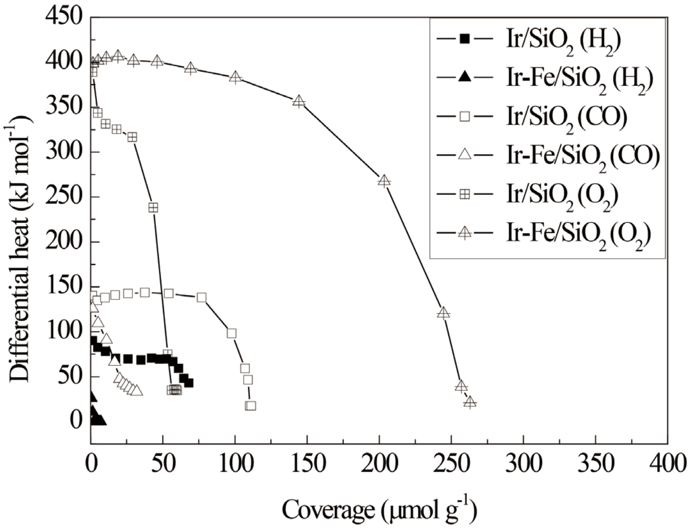

Figure 3. Differential heat curves vs. coverage of H_2, CO, and O_2 adsorbed separately on the Ir/SiO_2 and IrFe/SiO_2 catalysts.

Table 1: The saturation uptakes and initial adsorption heat of CO, O_2, and H_2 on the freshly reduced IrFe and Ir/SiO_2 catalysts.

Absorbate		Differential heat (kJ mol^{-1})	Coverage (μmol g_{Cat}^{-1})
H_2	IrFe/SiO_2	25	-
	Ir/SiO_2	90	55
	IrFe/Al_2O_3	60	24
	Fe/Ir/Al_2O_3	45	27
	Ir/Fe/Al_2O_3	55	35
CO	IrFe/SiO_2	120	20
	Ir/SiO_2	140	108
	IrFe/Al_2O_3	140	58
	Fe/Ir/Al_2O_3	140	65
	Ir/Fe/Al_2O_3	146	75
O_2	IrFe/SiO_2	400	240
	Ir/SiO_2	389	55
	IrFe/Al_2O_3	404	205
	Fe/Ir/Al_2O_3	408	205
	Ir/Fe/Al_2O_3	428	210

2.3 Quasi in situ ^{57}Fe Mössbauer spectroscopic studies

2.3.1 Comparison of IrFe/SiO_2 with Fe/SiO_2 treated with H_2 or O_2

Figure 4a displayed the ^{57}Fe Mössbauer spectra of the IrFe/SiO_2 catalyst after calcination, H_2 reduction, and re-oxidation by O_2, while Figure 4b showed the spectra of the Fe/SiO_2 sample treated under similar conditions for comparison. The corresponding Mössbauer parameters were listed in Table 2. The IS value, which is a very important factor for diagnosing the valence of Fe species [40], less than 0.40 mm s^{-1} could be ascribed to Fe^{3+}, and more than 0.95 mm s^{-1} was assigned to Fe^{2+} in the present study. In this case, it is reasonable that the Fe component with IS = 0.42 ~ 0.58 mm s^{-1} should be assigned to the intermediate valent state between Fe^{2+} and Fe^{3+}, i.e. Fe^{n+} ($2 < n < 3$). For IrFe/SiO_2 after calcination (Figure 4a), the spectrum was composed of a doublet and a sextuplet, which could be ascribed to superparamagnetic and large particles of α-Fe_2O_3, respectively. After reduction by H_2, the spectrum consisted of a doublet (IS = 0.58 mm s^{-1} and QS = 0.71 mm s^{-1}) for Fe^{n+} ($2 < n < 3$), a doublet (IS = 1.13 mm s^{-1} and QS = 2.15 mm s^{-1}) for Fe^{2+} strongly interacted with the SiO_2 support

[41], a sextuplet for Fe^0, and a singlet for FeIr alloy. These results were consistent with those reported in the literatures [42-44]. It is obvious that H_2 reduction at 300 °C reduced Fe^{3+} species to the low-valence iron species. When the reduced catalyst was treated by 1 % O_2 at 80 °C for 1 h, the spectrum (Figure 5c and Table 2) was consisted of Fe^{3+} (76 %) and Fe^0 (24 %). The disappearance of Fe^{n+} ($2 < n < 3$), Fe^{2+}, and FeIr alloy after O_2 oxidation suggested that the low-valence Fe species in the reduced IrFe/SiO_2 catalyst could be re-oxidized easily. It should be noted that there was still 24% Fe^0 maintained in the IrFe/SiO_2 catalyst even after the oxygen re-oxidation at 80 °C. As Wang et al. [45] reported, an iron/iron-oxide structure could be found for particles larger than the size of ~8 nm, it seemed that the cores of the Fe^0 particles remained as Fe^0, while the shell of Fe^0 particles were oxidized to Fe^{3+} after O_2 oxidation at 80 °C.

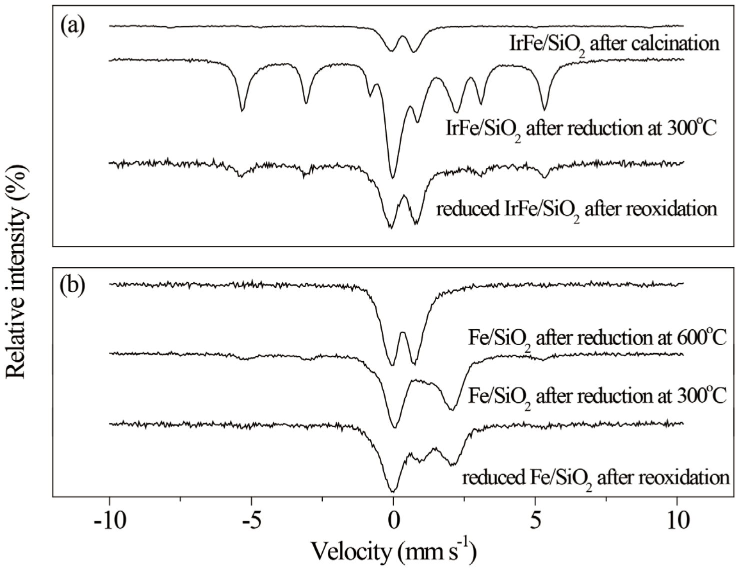

Figure 4. Quasi in situ ^{57}Fe Mössbauer spectra of IrFe/SiO_2 (a) before and after 100 % H_2 reduction at 300 °C for 2 h, and followed by 1 % O_2 treatment at 80 °C for 1 h, and Quasi in situ ^{57}Fe Mössbauer spectra of Fe/SiO_2 (b) after 100 % H_2 reduction at 300 °C for 2 h, after 100 % H_2 reduction at 600 °C for 2 h, and followed by 1 % O_2 treatment at 80 °C for 1 h after reduction at 600 °C.

As shown in Figure 4b and Table 2, the spectrum of Fe/SiO_2 after the H_2 reduction at 300 °C still showed a Fe^{3+} doublet, which was quite different from that of the IrFe/SiO_2 catalyst. Figure 4b indicated that only when Fe/SiO_2 was reduced at 600 °C, the low-valence Fe species including Fe^{n+}, Fe^0, Fe^{2+} (1) (IS = 1.10 mm s^{-1} and QS = 2.25 mm s^{-1}), and Fe^{2+} (2) (IS = 1.06 mm s^{-1} and QS = 1.69 mm s^{-1}) could be detected. Furthermore, the amount of Fe^0 in Fe/SiO_2 was significantly lower than that in IrFe/SiO_2, which indicated that the presence of Ir in IrFe/SiO_2 facilitated the reduction of Fe specie [35]. When the 600 °C reduced Fe/SiO_2 sample was treated by O_2 at 80 °C for 1 h, Fe^0 disappeared while Fe^{n+} was oxidized to Fe^{3+}. The disappearance of Fe^0 in the 600 °C reduced Fe/SiO_2 sample indicated that the particle size of Fe^0 in Fe/SiO_2 was possibly smaller than that in the 300 °C reduced IrFe/SiO_2 catalyst [45]. Moreover, Fe^{2+} (1) increased at the expense of Fe^{2+} (2), and the total amount of Fe^{2+} was almost unchanged, indicating that the low-valence Fe species (especially Fe^{2+}) in Fe/SiO_2 was more difficult to be reoxidized than those in IrFe/SiO_2. Therefore, the Fe species in IrFe/SiO_2 are more reactive towards H_2 reduction and O_2 re-oxidation than that in Fe/SiO_2.

2.3.2 Mössbauer spectra of IrFe/SiO_2 catalyst treated with reactant gas mixtures

The resulting ^{57}Fe Mössbauer spectra of the reduced IrFe/SiO_2 catalyst after treatment under different reactant gas mixtures at 80 °C for 1 h are shown in Figure 5, and the corresponding parameters are shown in Table 3. As shown in Figure 5a, all the low-valence iron components, including Fe^{n+}, Fe^{2+}, and FeIr alloy, were maintained when O_2 and H_2 were present simultaneously, indicating that H_2 could stabilize the low-valence iron components. Compared with the reduced IrFe/SiO_2 catalyst, the subsequent treatment with a mixture of H_2 and O_2 caused changes of the relative amounts of Fe^{n+}, Fe^{2+}, Fe^0, and FeIr alloy components, and a decrease of the IS values of Fe^{n+}, i.e. 0.58 mm s^{-1} (100 %) > 0.48 mm s^{-1} (40 %) > 0.42 mm s^{-1} (2 %). This result showed that these intermediate iron components had the tendency towards the lower oxidation states with increasing H_2 fractions in the feed gas mixture. When the

Table 2: ^{57}Fe Mössbauer parameters of the reduced and re-oxidized IrFe and Fe/SiO$_2$ catalysts

Treatment	Chemical state	IS[a] (mm s^{-1})	QS[b] (mm s^{-1})	MF[c] (T)	RI[d] (%)
IrFe/SiO$_2$					
Calcination at 300 °C for 5 h	Fe^{3+} (sp[e])	0.33	0.87	-	87
	Fe^{3+} (mg[f])	0.36	0.40	52.0	13
H$_2$ reduction at 300 °C for 2 h	Fe^{n+} ($2 < n < 3$)	0.58	0.71	-	20
	Fe^0	0.00	0.00	32.9	43
	Fe^{2+}	1.13	2.15	-	26
	FeIr	-0.11	-	-	11
1 % O$_2$ at 80 °C for 1 h	Fe^{3+}	0.34	0.94	-	76
	Fe^0	0.00	0.00	33.0	24
Fe/SiO$_2$					
Reduction at 300 °C for 2 h	Fe^{3+}	0.34	0.87	-	100
Reduction at 600 °C for 2 h	Fe^{n+} ($2 < n < 3$)	0.53	1.38	-	29
	Fe^0	0.00	0.00	32.4	10
	Fe^{2+} (1)	1.10	2.25	-	30
	Fe^{2+} (2)	1.06	1.69	-	31
1 % O$_2$ at 80 °C for 1 h	Fe^{3+}	0.35	0.92	-	44
	Fe^{2+} (1)	0.98	2.40	-	40
	Fe^{2+} (2)	0.95	1.73	-	16
IrFe/Al$_2$O$_3$					
Reduction at 300 °C for 2 h	Fe^{n+}	0.43	1.00		15
	Fe^0	0.00	0.00	33.4	31
	Fe^{2+}(a)	1.00	2.38		15
	FeIr	0.09	-		4
	Fe^{2+}(b)	1.04	1.55		35
1 % O$_2$ at 80 °C for 1 h	Fe^{3+}	0.33	1.08		80
	Fe^0	0.00	0.00	33.4	20
Fe/Ir/Al$_2$O$_3$					
Reduction at 300 °C for 2 h	Fe^{n+}	0.47	0.85		27
	Fe^0	0.00	0.00	33.3	18
	Fe^{2+}(a)	1.02	2.4		20
	Fe^{2+}(b)	0.99	1.67		35
1 % O$_2$ at 80 °C for 1 h	Fe^{3+}	0.32	1.09		80
	Fe^0	0.00	0.00	33.3	13
	Fe^{2+}(a)	1.07	2.14		6
Ir/Fe/Al$_2$O$_3$					
Reduction at 300 °C for 2 h	Fe^{3+}	0.36	1.14		24
	Fe^{2+}(a)	1.09	2.22		29
	Fe^{2+}(b)	1.02	1.56		47
1 % O$_2$ at 80 °C for 1 h	Fe^{3+}	0.32	1.08		81
	Fe^{2+}(a)	1.09	2.15		19

[a] IS, isomer shift; [b] QS, electric quadrupole splitting; [c] MF, magnetic field; [d] RI, relative intensity; [e] sp, superparamagnetic; [f] mg, magnetic; Uncertainty is ± 5 % of reported value.

reduced IrFe/SiO$_2$ catalyst was treated by 2 % CO at 80 °C for 1 h, the relative amounts of Fe^0, Fe^{2+}, and FeIr alloy were almost identical to that treated by the mixture of 2 % H$_2$ and 1 % O$_2$, and the Mössbauer spectrum were almost the same. Since CO could possibly be dissociated to carbon and oxygen atoms on Fe^0 [46], the oxygen atoms could react with Fe^0 atom and formed iron oxide, resulting in higher iron valence states.

Table 3: ^{57}Fe Mössbauer parameters of the IrFe catalysts after the PROX reaction.

Sample	Chemical state	IS[a] (mms^{-1})	QS[b] (mms^{-1})	H[c] (T)	RI[d] (%)
40 % H_2 + 2 % CO +1 % O_2 at 80 °C for 1 h on IrFe/SiO_2	Fe^{3+}	0.35	0.92	-	54
	Fe^0	0.00	0.00	32.9	28
	Fe^{2+}	1.12	2.16	-	18
10 % H_2 + 2 % CO +1 % O_2 at 80 °C for 1 h on IrFe/SiO_2	Fe^{3+}	0.35	0.92	-	56
	Fe^0	0.00	0.00	32.9	27
	Fe^{2+}	1.10	2.16	-	17
2 % H_2 + 2 % CO +1 % O_2 at 80 °C for 1 h on IrFe/SiO_2	Fe^{3+}	0.36	0.92	-	60
	Fe^0	0.00	0.00	32.9	26
	Fe^{2+}	1.10	2.15	-	14
2 % CO +1 % O_2 at 80 °C for 1 h on IrFe/SiO_2	Fe^{3+}	0.34	0.95	-	67
	Fe^0	0.00	0.00	32.9	29
	Fe^{2+}	1.11	2.13	-	4
10 % H_2O + 2 % CO +1 % O_2 at 80 °C for 1 h on IrFe/SiO_2	Fe^{3+}	0.36	0.66	-	86
	Fe^{2+}	1.04	2.34	-	14
40 % H_2 + 2 % CO +1 % O_2 at 80 °C for 1 h on IrFe/Al_2O_3	Fe^{3+}	0.32	1.09		61
	Fe^0	0.00	0.00	33.4	22
	Fe^{2+}(a)	1.10	2.10		17
40 % H_2 + 2 % CO +1 % O_2 at 80 °C for 1 h on Fe/Ir/Al_2O_3	Fe^{3+}	0.32	1.10		70
	Fe^0	0.00	0.00	33.3	15
	Fe^{2+}(a)	1.08	2.11		15
40 % H_2 + 2 % CO +1 % O_2 at 80 °C for 1 h on Ir/Fe/Al_2O_3	Fe^{3+}	0.31	1.11		78
	Fe^{2+}(a)	1.11	2.06		22

[a] IS, isomer shift; [b] QS, electric quadrupole splitting; [c] MF, magnetic field; [d] RI, relative intensity; [e] sp, superparamagnetic; [f] mg, magnetic; Uncertainty is ± 5 % of reported value.

When the reduced IrFe/SiO_2 catalyst was exposed to the feed gas mixture of CO, O_2, and H_2 (0 ~ 40 %) at 80 °C for 1 h, as shown in Figure 5b, all the spectra consisted of Fe^0, Fe^{2+}, and α-Fe_2O_3, and both the intermediate iron species (Fe^{n+}) and FeIr alloy disappeared completely. With an increase of H_2 concentration from 0 to 40 %, the amount of Fe^{3+} decreased and the amount of Fe^{2+} increased from 4 to 18 %. In the mean time, the amount of Fe^0 was stable around 28 % for 0 ~ 40 % H_2 concentrations contained in the feed gas mixtures. Although the reduced IrFe/SiO_2 catalyst contained 43 % Fe^0, the subsequent treatment with either 1 % O_2 or different feed gas mixtures could oxidize only a part of Fe^0, always leaving ~ 25 % Fe^0 intact in IrFe/SiO_2. According to the literature[43], it was probably that this part of Fe^0 was encapsulated by the ferric oxide, and might be not take part in the CO oxidation or PROX reactions.

The reaction rate and the concentration of different Fe species in the IrFe/SiO_2 catalyst have been plotted as a function of H_2 concentration, as shown in Figure 6. Fe^{3+} decreased with the increasing H_2 concentration, while the concentration of Fe^0 kept steady at 25 ~ 28%. Fe^{2+} increased with the increase of H_2 concentration from 0 to 10 % and then leveled off at higher H_2 concentrations, which was consistent with the change of the reaction rate for CO oxidation. This suggested that the Fe^{2+} amount had a close relation with the CO oxidation rate, and the Fe^{2+} concentration depended on the H_2 concentration in the reactant gas. Similarly,

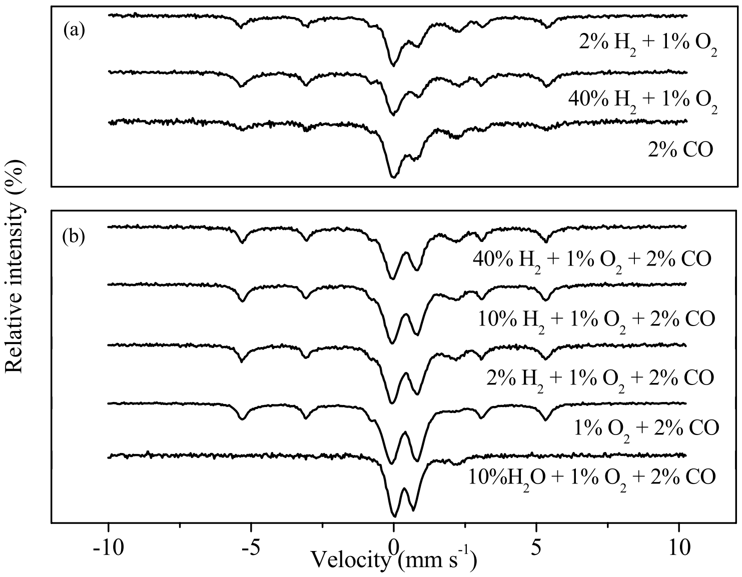

Figure 5. Quasi in situ ^{57}Fe Mössbauer spectra of the reduced IrFe/SiO$_2$ catalyst after treatment in different atmospheres at 80 °C for 1 h.

many literatures reported that the middle valence metal oxide played the role of O_2 activation in the promoted noble metal catalysts, such as the PtFe catalyst [13], PtSn catalysts [11], and Cu/CeO$_2$ catalyst [47]. The correlation between Fe^{2+} amount determined by Mössbauer spectroscopy and the CO oxidation rate indicated that Fe^{2+} might play the role of O_2 activation during the PROX reaction. In addition, as shown in Table 3, the IrFe/SiO$_2$ catalyst treated by the gas mixture of 10 % H_2O, 2 % CO, and 1 % O_2 was composed of Fe^{3+} and Fe^{2+}, and the Fe^{2+} amount was the same as that after being treated by the mixture of 2 % H_2, 2 % CO, and 1 % O_2. This result indicated again that the Fe^{2+} species played the role of activating O_2, and either H_2 43 or H_2O in the feed gas could stabilize the Fe^{2+} species. The absence of Fe^0 suggested that Fe^0 was oxidized to either Fe^{3+} or Fe^{2+}. It should be noted here that the Fe^{3+} species with IS = 0.36 mm s^{-1} and QS = 0.66 mm s^{-1} could be ascribed to Fe^{3+} in ferrihydrite 48, which might be different from the superparamagnetic α-Fe$_2$O$_3$ (IS = 0.32 ~ 0.36 mm s^{-1} and QS = 0.87 ~ 0.94 mm s^{-1}). OH groups of the ferrihydrite might also participate in the PROX reaction [49,50].

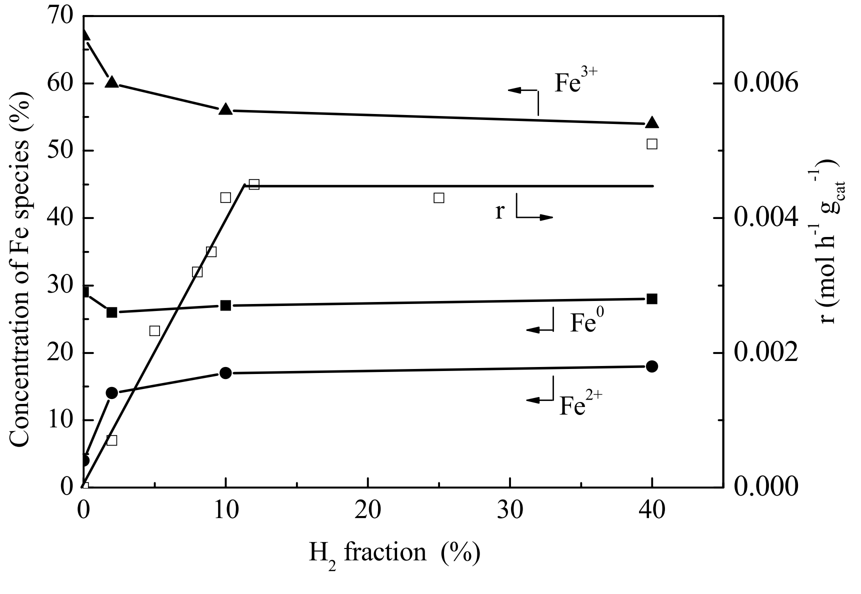

Figure 6. Plots of the amounts of different Fe species and CO oxidation rate (r) against H_2 fractions in the feed gas mixtures.

As stated in Part 3.3.1, Ir facilitates the reduction of Fe^{3+} and the addition of Fe greatly enhances O_2 adsorption, suggesting that the low valence Fe species in the $IrFe/SiO_2$ catalyst could activate O_2 and could be regenerated by H_2 or H_2O at low temperatures. It should be noted that Ir and Fe species must be in intimate contact with each other, aiming at the easier hydrogen spillover from Ir to Fe. The disappearance of FeIr alloy in the reactant atmosphere indicated that it was possible that the active Fe^{2+} species came from the oxidation of FeIr alloy, forming intimately contacted Fe^{2+} species and Ir particles. Similar conclusions had been drawn on the $PtSn/SiO_2$ catalyst by Margitfalvi et al [51], which suggested that a PtSn $\leftrightarrow$ Sn^{4+} + Pt reaction took place in CO oxidation. Apart from this part of Fe^{2+} coming from FeIr alloy, the vanishing part of Fe^0 might also be transformed into Fe^{2+} in the reactant atmosphere as long as it was in close contact with the Ir particles, and this part of Fe^{2+} might also serve as the active site for O_2 activation. However, it was probably that Fe^{n+} in the reduced $IrFe/SiO_2$ catalyst was oxidized into high valence Fe^{3+} rather than Fe^{2+} in the reaction atmosphere, and Fe^{2+} species could not originated from Fe^{n+} species. According to the discussions above, Ir served as the sites for activating CO while Fe^{2+} for activating O_2, and the PROX reaction over the $IrFe/SiO_2$ catalyst proceeded via a non-competitive Langmuir-Hinshelwood reaction route. The presence of H_2 could stabilize Fe^{2+} sites for the PROX reaction, and furthermore, increase the CO conversion.

3. PROX over $IrFe/Al_2O_3$

3.1 Catalytic activity - the effect of impregnation series

Three different $IrFe/Al_2O_3$ catalysts were prepared by different impregnation methods. The $IrFe/Al_2O_3$ catalyst was prepared by co-impregnation method. The $Ir/Fe/Al_2O_3$ catalyst was first impregnated with an aqueous mixture of $Fe(NO_3)_3$ and $^{57}Fe(NO_3)_3$, and then Ir was deposited on the Fe/Al_2O_3. $Fe/Ir/Al_2O_3$ catalyst was prepared with an inverse impregnation sequence. The catalytic PROX performances of the catalysts were shown in Figure 7. Both the activity and the selectivity toward CO followed the order of $IrFe/Al_2O_3$ > $Fe/Ir/Al_2O_3$ > $Ir/Fe/Al_2O_3$.

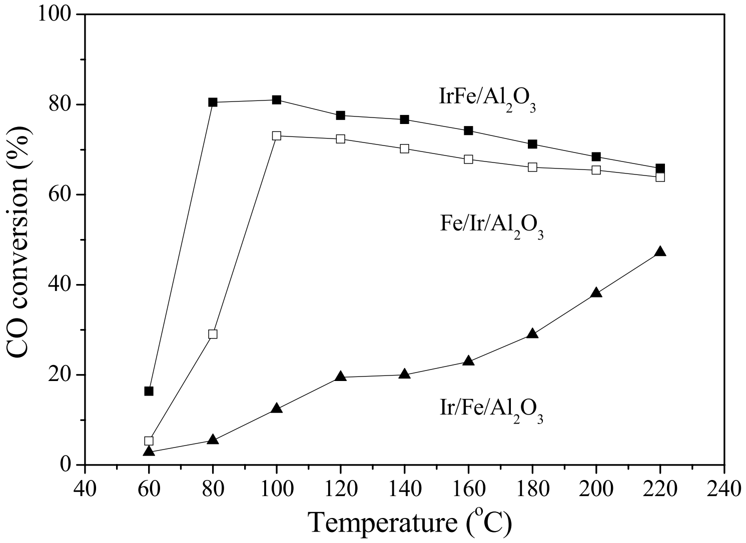

Figure 7. CO conversion vs. reaction temperature over the $IrFe/Al_2O_3$ (■), $Fe/Ir/Al_2O_3$ (□), and $Ir/Fe/Al_2O_3$ (▲) catalysts.

3.2 The activation of O_2

H_2, CO, and O_2 adsorption behavior on the three reduced catalysts by microcalorimetric study were shown in Figure 8 and Table 1. The differences in the saturation uptakes and the initial heat of CO were not significant on the three IrFe catalysts, which indicated that the effect of CO adsorption on the activity could be neglected. Additionally, the saturation uptakes and the initial heat of O_2 were almost identical on the three catalysts. The results of microcalorimetric study on CO and O_2 demonstrated that the adsorption properties of the three IrFe catalysts were almost the same, and thus, the adsorption could not lead to the different PROX activities.

3.3 Quasi in situ Mössbauer spectroscopic study

3.3.1 Comparison of different IrFe catalysts treated with H_2

Quasi in situ ^{57}Fe Mössbauer spectra of the three IrFe catalysts after reduction by H_2 were

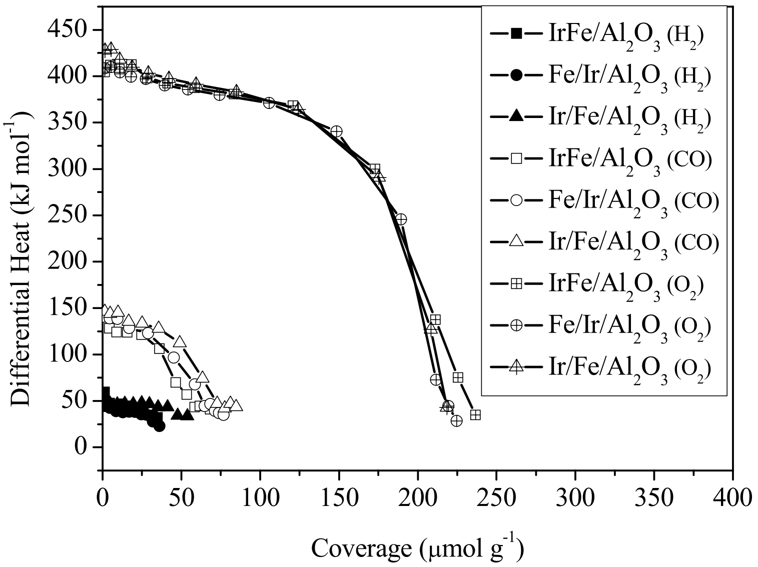

Figure 8. Differential heat curves vs. coverage of H_2, CO, and O_2 adsorbed on the IrFe/Al_2O_3, Fe/Ir/Al_2O_3 and Ir/Fe/Al_2O_3 catalysts.

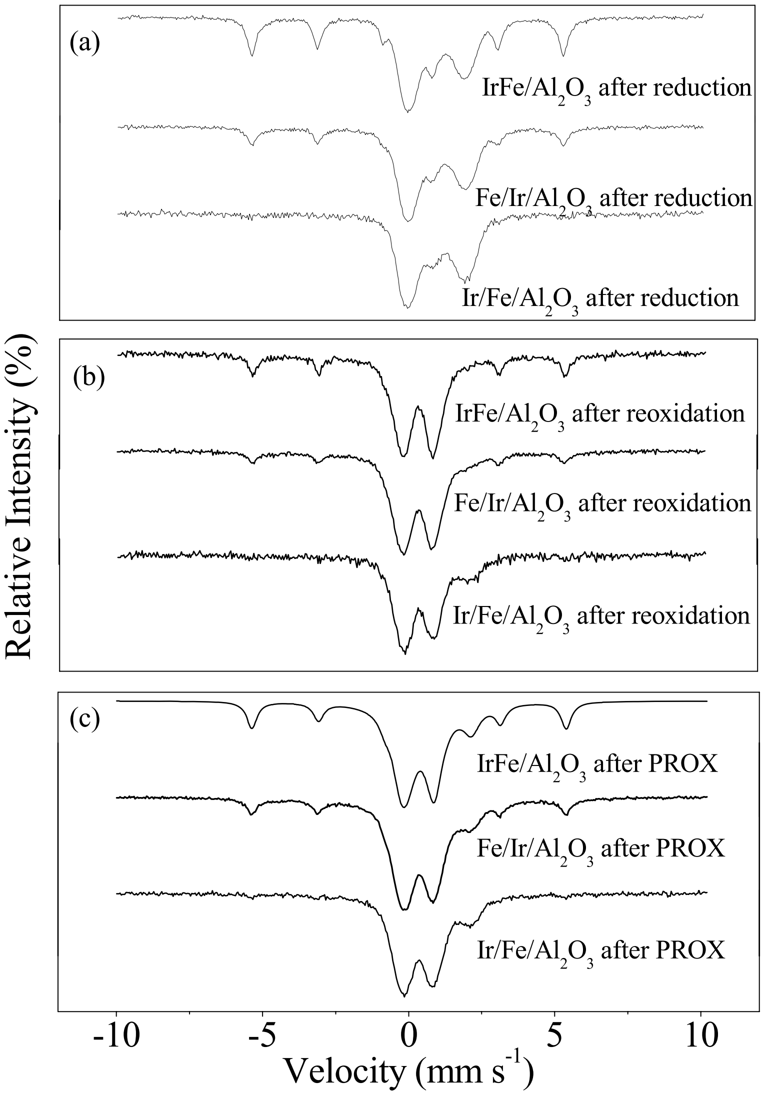

Figure 9. Quasi in situ ^{57}Fe Mossbauer spectra of the IrFe/Al_2O_3, Fe/Ir/Al_2O_3, and Ir/Fe/Al_2O_3 catalysts after H_2 reduction at 300 °C for 2 h (a), O_2 re-oxidation at 80 °C for 1 h (b), and the PROX reaction at 80 °C for 1 h (c).

shown in Figure 9a and Table 2, which showed great differences in the composition of the IrFe catalysts, indicating that the impregnation sequence had a close relation with the reducibility. Similar to the spectra of the reduced IrFe/SiO_2 catalyst, the doublet (IS = 0.58 mm s^{-1} and QS = 0.71 mm s^{-1}) could be ascribed to Fe^{n+} ($2 < n < 3$), and the six-line component with the isomer shift (IS = 0.00), the quadrupole constant (QS = 0.00), and a magnetic splitting (MF = 33.3 T) could be ascribed to α-Fe^0. Fe^0 in the three reduced IrFe/Al_2O_3 catalysts were not in highly dispersed state; instead, Fe^0 had a large particle size. The two doublets, which had similar isomer shifts but different quadrupole splittings (QS = 2.38 mm s^{-1} and QS = 1.55 mm s^{-1}), could be ascribed to two different kinds of Fe^{2+} (Fe^{2+} (a) and Fe^{2+} (b), respectively) in different positions in the aluminates. The spectra of the reduced IrFe/Al_2O_3 catalyst showed the presence of Fe^{n+}, α-Fe^0, two kinds of Fe^{2+}, and FeIr alloy. However, no FeIr alloy was observed on the reduced Fe/Ir/Al_2O_3, and the amount of Fe^0 is less than that in IrFe/Al_2O_3. The spectra of the reduced Ir/Fe/Al_2O_3 showed the presence of Fe^{3+}, and two kinds of Fe^{2+} species. The Mössbauer results showed that the different impregnation sequences during the preparation procedure influenced the reducibility of the Fe species. Moreover, the reducibility of the Fe species followed the order of IrFe/Al_2O_3 > Fe/Ir/Al_2O_3 > Ir/Fe/Al_2O_3, which was identical with the trend of the PROX activity.

3.3.2 Comparison of different IrFe catalysts treated with O_2

Mössbauer experiments of the three reduced IrFe catalysts after being treated by O_2 at 80 °C were also conducted. As seen in Figure 9b, Fe^0 were still present as they could not be oxidized to Fe^{3+} or Fe^{2+}. Similar to Ir-Fe/SiO_2, it was proposed on Ir/Fe/Al_2O_3 and Fe/Ir/Al_2O_3 that only the outer layers of the Fe^0 particles had been oxidized when treated by 1 % O_2, whereas the cores of Fe^0 were covered by Fe oxide species and were maintained in the oxidant atmosphere. Analogously, Fe^{2+}(a) species was also retained in O_2 atmosphere in Ir/Fe/Al_2O_3 and Fe/Ir/Al_2O_3, which could be attributed to the strong interaction between Fe species and Al_2O_3, or to the encapsulation of Fe^{2+} by Fe^{3+} oxide. This was similar to Fe/SiO_2, on which the interaction between Fe^{2+} and SiO_2 could stabilize the Fe^{2+} species after being treated by O_2. However, if Fe^{2+} species was too stable to be reoxidized in O_2 atmosphere, this part of Fe^{2+} could not play the part of activating O_2. Therefore, it was reasonable to infer that not all of Fe^{2+}(a) was active for O_2 adsorption on Ir/Fe/Al_2O_3 and Fe/Ir/Al_2O_3 at 80 °C, and the active sites for O_2 activation were probably part of Fe^{2+} (a), Fe^{2+} (b), and Fe^0 for Ir–Fe/Al_2O_3 and Fe/Ir/Al_2O_3, and Fe^{2+} (a) or Fe^{2+} (b) for Ir/Fe/Al_2O_3, respectively.

3.3.3 Mössbauer spectra of IrFe catalysts treated with reactant gas mixtures

Mössbauer results of the three IrFe/Al_2O_3 catalysts after PROX reaction were shown in Figure 9c and Table 3. IrFe/Al_2O_3 and Fe/Ir/Al_2O_3 were consisted of Fe^0, Fe^{2+} (a), and Fe^{3+}. The treatment of the reduced catalysts by the PROX gas converted Fe^{2+} (b) and FeIr alloy to Fe^{3+} completely, and the amount of Fe^{2+} (a) and Fe^0 decreased in the mean time. Therefore, Fe^0 and Fe^{2+} (a) might be the active sites for O_2 activation for the IrFe/Al_2O_3 and Fe/Ir/Al_2O_3 catalysts. However, the amount of Fe^0 after PROX reaction were almost the same with that after O_2 treatment, indicating that Fe^0 species were encapsulated by Fe^{2+} or Fe^{3+} species and could not activate O_2. In addition, when Ir/Fe/Al_2O_3 was treated by the PROX gas, Fe^{2+} (b) was oxidized to Fe^{3+} completely, and the amount of Fe^{2+} (a) decreased. Therefore, it could be inferred that Fe^{2+} (a) was active for O_2 activation for the three IrFe/Al_2O_3 catalysts.

To verify this conclusion, the relation between the amount of the active Fe^{2+} (a) and CO conversion were plotted in Figure 10. As discussed above, only a part of Fe^{2+} (a) was active for O_2 activation, so the amount of the active Fe^{2+} (a) could be calculated by the following equation:

$$n_{Fe^{2+}(a),\text{active}} = n_{Fe^{2+}(a),\text{ after reaction}} - n_{Fe^{2+}(a),\text{after oxidation}}$$

where $n_{Fe^{2+}(a),\text{active}}$ was the amount of the active Fe^{2+} (a), $n_{Fe^{2+}(a),\text{ after reaction}}$ was the amount of Fe^{2+} (a) after PROX reaction, and $n_{Fe^{2+}(a),\text{after oxidation}}$ was the amount of Fe^{2+} (a) after O_2 reoxidation. Therefore, the amount of the active Fe^{2+} (a) for IrFe/Al_2O_3, Fe/Ir/Al_2O_3, and Ir/Fe/Al_2O_3 were calculated as 17, 9, and 3% respectively. It can be seen clearly in Figure 10 that CO conversion was proportional to the amount of Fe^{2+} (a). After the PROX reaction, the amount of the active Fe^{2+} (a) for O_2 activation followed the order of IrFe/Al_2O_3 > Fe/Ir/Al_2O_3 > Ir/Fe/Al_2O_3, and this trend was identical with that of CO conversion, suggesting again that Fe^{2+} (a) in IrFe catalysts was the active site for the PROX reaction.

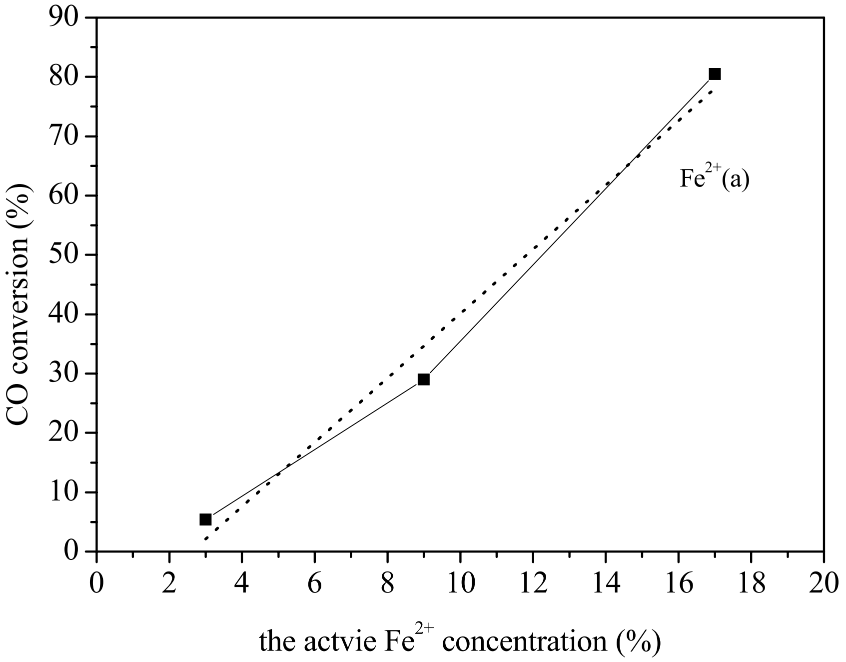

Figure 10. Plot of CO conversions in PROX reaction stream against the amounts of the active Fe^{2+} (Fe^{2+} (a)) concentration determined by ^{57}Fe Mössbauer spectroscopy.

4. Summary

By using quasi in situ Mössbauer spectroscopy, a clear picture had been given about the change of the amount of different Fe species with different H_2 concentrations and impregnation sequences in the IrFe bimetallic catalysts during the PROX reaction. Quasi in situ Mössbauer spectroscopy provided the important information of the distribution of different Fe species on the catalyst surface and bulk under the reaction conditions, which is difficult to be achieved by other techniques. The main conclusions are as follows:

1) With the help of Ir, Fe^{3+} in the IrFe catalyst could be easily reduced to low valence Fe species, including Fe^{n+} ($2 < n < 3$), Fe^0, Fe^{2+}, and FeIr alloy, and the low valence Fe species could also be easily re-oxidized when being treated by O_2.

2) Fe^{n+} ($2 < n < 3$) was oxidized into Fe^{3+} in the PROX gas mixture, so it was not active for the PROX reaction. Meanwhile, part of Fe^0 particles was retained in the PROX reaction probably due to its large particle size and the encapsulation by other Fe species. Therefore, Fe^0 could not be the active site for activating O_2.

3) For the IrFe/SiO_2 catalyst, the amount of Fe^{2+} species increased when the H_2 fraction was increased in the PROX gas mixtures, and this trend was consistent with that of the CO conversion. For the IrFe/Al_2O_3 catalyst, the impregnation sequences influenced the amount of the active Fe^{2+}, i.e., Fe^{2+}(a), and the CO oxidation rate increased with the amount of Fe^{2+} (a) species. Both the Mössbauer results on the IrFe/SiO_2 and IrFe/Al_2O_3 catalysts suggested that Fe^{2+} species was the active site for activating O_2.

4) H_2 in the PROX gas mixtures accelerated the PROX reaction by stabilizing Fe^{2+} species in the IrFe/SiO_2 catalyst, and the impregnation sequences influenced the PROX activity by changing the amount of the active Fe^{2+} species in the IrFe/Al_2O_3 catalyst.

5) The adsorption of CO was weakened, while the adsorption of O_2 was strengthened by the addition of Fe in the Ir/SiO_2 catalyst. Therefore, it was probably that the PROX reaction followed a non-competitive Langmuir-Hinshelwood mechanism where O_2 was activated on Fe^{2+} and CO was adsorbed on the intimately contacted Ir sites. Similar conclusion could be drawn on the IrFe/Al_2O_3 catalyst.

6) For the IrFe/SiO_2 catalyst, when the reduced IrFe catalyst were subjected to the PROX gas mixture, FeIr alloy segregated and formed Fe^{2+} and Ir particles, which were active for PROX reaction. Although FeIr alloy in the IrFe/SiO_2 catalyst could segregate into intimate contacted Ir and Fe^{2+} species for activating CO and O_2 respectively, few FeIr alloy was formed in the three reduced IrFe/Al_2O_3 catalysts, probably due to the stronger metal-support interaction between Fe and Al_2O_3 than that of Fe and SiO_2, and FeIr alloy might not be necessary for the PROX reaction on the IrFe/Al_2O_3 catalyst.

7) The IrFe/Al_2O_3 catalysts were similar to Fe/

SiO_2, on which the interaction between Fe^{2+} species and the supports could stabilize the Fe^{2+} species even after being treated by O_2. The two doublets, which had similar isomer shifts but different quadrupole splittings, could be ascribed to two kinds of Fe^{2+} species in different positions in the supports.

Acknowledgement

Financial supports from Chinese Academy of Sciences for "100 Talents" project, the National Natural Science Foundation of China (No. 11079036) and the Natural Science Foundation of Liaoning Province (No. 20092173) are greatly acknowledged.

References

[1] A. Sirijaruphan, J. G. Jr. Goodwin, R. W. Rice: Investigation of the initial rapid deactivation of platinum catalysts during the selective oxidation of carbon monoxide, *J. Catal.* **2004**, *221*, 288.

[2] G. Sedmak, S. Hočevar, J. Levec: Kinetics of selective CO oxidation in excess of H_2 over the nanostructured $Cu_{0.1}Ce_{0.9}O_{2-(y)}$ catalyst, *J. Catal.* **2003**, *213*, 135.

[3] W. B. Kim, T. Voitl, G. J. Rodriguez-Rivera, S. T. Evans, J. A. Dumesic: Preferential oxidation of CO in H_2 by aqueous polyoxometalates over metal catalysts, *Angew. Chem. Int. Ed.* **2005**, *44*, 778.

[4] O. Pozdnyakove-Tellinger, D. Teschner, J. Kröhnert, F. C. Jentoft, A. Knop-Gericke, R. Schlögl, A. Wootsch: Surface water-assisted preferential CO oxidation on Pt/CeO_2 catalyst, *J. Phys. Chem. C* **2007**, *111*, 5426.

[5] W. Li, F. J. Gracia, E. E. Wolf: Selective combinatorial catalysis challenges and opportunities: the preferential oxidation of carbon monoxide, *Catal. Today* **2003**, *81*, 437.

[6] E. Şimşek, Ş. Özkara, A. E. Aksoylu, Z. I. Önsan: Preferential CO oxidation over activated carbon supported catalysts in H_2-rich gas streams containing CO_2 and H_2O, *Appl. Catal. A* **2007**, *316*, 169.

[7] B. T. Qiao, A. Q. Wang, X. F. Yang, L. F. Allard, Z. Jiang, Y. T. Cui, J. Y. Liu, J. Li, T. Zhang: Single-atom catalysis of CO oxidation using Pt_1/FeO_x , *Nature Chem.* **2011**, *3*, 634.

[8] J. Yin, J. Wang, T. Zhang, X. D. Wang: Novel alumina-supported PtFe alloy nanoparticles for preferential oxidation of carbon monoxide in hydrogen, *Catal. Lett.* **2008**, *125*, 76.

[9] X. S. Liu, O. Korotkikh, R. Farrauto: Selective catalytic oxidation of CO in H_2: structural study of Fe oxide-promoted Pt/alumina catalyst, *Appl. Catal. A* **2002**, *226*, 293.

[10] M. Kotobuki, A. Watanabe, H. Uchida, H. Yamashita, M. Watanabe: Reaction mechanism of preferential oxidation of carbon monoxide on Pt, Fe, and Pt-Fe/mordenite catalysts, *J. Catal.* **2005**, *236*, 262.

[11] M. M. Schubert, M. J. Kahlich, G. Feldmeyer, M. Hüttner, S. Hackenberg, H. A. Gasteiger, R. J. Behm: Bimetallic PtSn catalyst for selective CO oxidation in H_2-rich gases at low temperatures, *Phys. Chem. Chem. Phys.* **2001**, *3*, 1123.

[12] A. Sirijaruphan, J. G. Goodwin Jr., R. W. Rice: Effect of Fe promotion on the surface reaction parameters of Pt/gamma-Al_2O_3 for the selective oxidation of CO, *J. Catal.* **2004**, *224*, 304.

[13] M. Kotobuki, T. Shido, M. Tada, H.Uchida, H. Yamashita, Y. Iwasawa, M. Watanabe: XAFS characterization of Pt-Fe/zeolite catalysts for preferential oxidation of CO in hydrogen fuel gases, *Catal. Lett.* **2005**, *103*, 263.

[14] Y. -N. Sun, Z. -H. Qin, M. Lewandowski, E. Carrasco, M. Sterrer, S. Shaikhutdinov, H. -J. Freund: Monolayer iron oxide film on platinum promotes low temperature CO oxidation, *J. Catal.* **2009**, *266*, 359.

[15] Q. Fu, W. X. Li, Y. X. Yao, H. Y. Liu, H. -Y. Su, D. Ma, X. -K. Gu, L. M. Chen, Z. Wang, H. Zhang, B. Wang, X. H. Bao: Interface-Confined Ferrous Centers for Catalytic Oxidation, *Science* **2010**, *328*, 1141.

[16] E. Quinet, F. Morfin, F. Diehl, P. Avenier, V. Caps, J. -L. Rousset: Hydrogen effect on the preferential oxidation of carbon monoxide over alumina-supported gold nanoparticles, *Appl. Catal. B* **2008**, *80*, 195.

[17] C. Rossignol, S. Arrii, F. Morfin, L. Piccolo, V. Caps, J. -L. Rousset: Selective oxidation of CO over model gold-based catalysts in the presence of H_2, *J. Catal.* **2005**, *230*, 476.

[18] E. Quinet, L. Piccolo, J. Daly, F. C. Meunier, F. Morfin, A. Valcarcel, F. Diehl, P. Avenier, V. Caps, J. -L. Rousset: H2-induced promotion of CO oxidation over unsupported gold , *Catal. Today* **2008**, *138*, 43.

[19] L. Piccolo, H. Daly, A. Valcarcel, F. C. Meunier: Promotional effect of H_2 on CO oxidation over Au/TiO_2 studied by operando infrared spectroscopy , *Appl. Catal. B* **2009**, *86*, 190.

[20] A. Sirijaruphan, J. G. Goodwin Jr., R. W. Rice, D. G. Wei, K. R. Butcher, G. W. Roberts, J. J. Spivey: Effect of metal foam supports on the selective oxidation of CO on Fe-promoted Pt/gamma-Al_2O_3, *Appl. Catal. A* **2005**, *281*, 11.

[21] D. H. Kim, M. S. Lim: Kinetics of selective CO oxidation in hydrogen-rich mixtures on Pt/alumina catalysts, *Appl. Catal. A* **2002**, *224*, 27.

[22] M. J. Kahlich, H. A. Gasteiger, R. J. Behm: Kinetics of the selective CO oxidation in H_2-rich gas on Pt/Al_2O_3, *J. Catal.* **1997**, *171*, 93.

[23] G. Jacobs, U. M. Graham, E. Chenu, P. M. Patterson, A. Dozier, B. H. Davis: Low-temperature water-gas shift: impact of Pt promoter loading on the partial reduction of ceria and consequences for catalyst design, *J. Catal.* **2005**, *229*, 499.

[24] A. B. Mhadeswar, D. G. Vlachos: Microkinetic modeling for water-promoted CO oxidation, water-gas shift, and preferential oxidation of CO on pt, *J. Phys. Chem. B* **2004**, *108*, 15246.

[25] F. J. Berry, *Mössbauer spectroscopy applied to inorganic chemistry* Plenum Press: New York, 1984 Vol. 1. p 391.

[26] L. Stievano: ^{193}Ir and ^{57}Fe Mössbauer characterisation of iridium/iron bimetallic catalysts for methanol synthesis, *Hyperfine Interact.* **2000**, *126*, 101.

[27] A. Fukuoka, T. Kimura, N. Kosugi, H. Kuroda, Y. Minai, Y. Sakai, T. Tominaga, M. Ichikawa: Bimetallic promotion of alcohol production in co hydrogenation and olefin hydroformylation on RHFE, PTFE, PDFE, and IRFE cluster-derived catalysts, *J. Catal.* **1990**, *126*, 434.

[28] Y. Y. Zhu, X. D. Wang, Y. Zhang, J. Wang, Y. Q. Huang, C. Kappenstein, T. Zhang: Effect of Ir crystallographic site on the catalytic performance of Ir-substituted barium hexaferrites for N_2O decomposition, *Appl. Catal. A-Gen.* **2011**, *409-410*, 194.

[29] Y. Y. Zhu, X. D. Wang, Y. Q. Huang, Y. Zhang, G. T. Wu, J. Wang, T. Zhang: Identification of the Crystallographic Sites of Ir in $BaIr_{0.2}FeAl_{10.8}O_{19}$ Hexaaluminate, *J. Phys. Chem. C* **2012**, *116*, 24487.

[30] Y. Y. Zhu, X. D. Wang, G. T. Wu, Y. Q. Huang, Y. Zhang, J. Wang, T. Zhang: Evolution of Fe Crystallographic Sites from Barium Hexaaluminate to Hexaferrite , *J. Phys. Chem. C* **2012**, *116*, 671.

[31] K. Nomura, E. Kuzmann, C. A. Barrero, S. Stichleutner, Z. Homonnay: ^{119}Sn Mössbauer study of sol-gel synthetized $Fe_xSb_ySn_{1-x-y}O_{2-\delta}$ powders, *Hyperfine Interact.* **2008**, *184*, 57.

[32] R. Y. Tang, S. Zhang, C. Y. Wang, D. B. Liang, L. W. Lin: An Insitu Combined Temperature-Programmed Reduction - Mössbauer-Spectroscopy of Alumina-Supported Iron Catalysts, *J. Catal.* **1987**, *106*, 440.

[33] W. S. Zhang, A. Q. Wang, L. Li, X. D. Wang, T. Zhang: Promoting role of Fe in the preferential oxidation of CO over Ir/Al_2O_3, *Catal. Lett.* **2008**, *121*, 319.

[34] W. S. Zhang, A. Q. Wang, L. Li, X. D. Wang, T. Zhang: Design of a novel bifunctional catalyst $IrFe/Al_2O_3$ for preferential CO oxidation, *Catal. Today* **2008**, *131*, 457.

[35] W. S. Zhang, Y. Q. Huang, J. Wang, K. Liu, X. D. Wang, A. Q. Wang, T. Zhang: $IrFeO_x/SiO_2$-A highly active catalyst for preferential CO oxidation in H_2, *Int. J. Hydrogen Energy* **2010**, *35*, 3065.

[36] K. Liu, A. Q. Wang, W. S. Zhang, J. Wang, Y. Q. Huang, J. Y. Shen, T. Zhang: Quasi In Situ ^{57}Fe Mössbauer Spectroscopic Study: Quantitative Correlation between Fe^{2+} and H_2 Concentration for PROX over $Ir-Fe/SiO_2$ Catalyst, *J. Phys. Chem. C* **2010**, *114*, 8533.

[37] K. Liu, A. Q. Wang, W. S. Zhang, J. Wang, Y. Q. Huang, C. Z. Jin, J. Y. Shen, T. Zhang: ^{57}Fe Mössbauer Spectroscopy of Ir-Fe Catalysts for Preferential CO Oxidation in H_2, *Chin. J. Catal.* **2010**, *31*, 1335.

[38] A. Manasilp, E. Gulari: Selective CO oxidation over Pt/alumina catalysts for fuel cell applications, *Appl. Catal. B* **2002**, *37*, 17.

[39] H. Igarashi, T. Fujino, Y. Zhu, H. Uchida, M. Watanabe: CO Tolerance of Pt alloy electrocatalysts for polymer electrolyte fuel cells and the detoxification mechanism, *Phys. Chem. Chem. Phys.* **2001**, *3*, 306.

[40] E. Murad, J. Cashion, *Mössbauer Spectroscopy of Environmental Materials and their industrial utilization* Kluwer Academic Publishers: Massachusetts, 1984 p 19.

[41] V. R. Balse, W. M. H. Sachtler, J. A. Dumesic: Mössbauer spectroscopy studies of PtFe/NaY zeolite, Catal. Lett. 1988, *1*, 275.

[42] L. M. P. Van Gruijthuijsen, G. J. Howsmon, W. N. Delgass, D. C. Koningsberger, R. A. Van Santen, J. W. Niemantsverdriet: Structure and reactivity of bimetallic $FeIr/SiO_2$ catalysts after reduction and during high-pressure CO hydrogenation, *J. Catal.* **1997**, *170*, 331.

[43] J. W. Niemantsverdriet, A. M. Van Der Kraan: Characterization of Supported Bimetallic Feir SiO_2 Catalysts by Mössbauer-Spectroscopy, Temperature-Programmed Reduction and X-Ray Photoelectron-Spectroscopy, *Surf. Interface Anal.* **1986**, *9*, 221.

[44] F. J. Berry, S. Jobson: A Mössbauer Spectroscopic Investigation of the Influence of Iridium on the Changes Induced in Iron-Iridium Catalysts when Treated in Hydrogen and in Carbon-Monoxide and Hydrogen, *Hyperfine Interact.* **1988**, *41*, 745.

[45] C. M. Wang, D. R. Baer, L. E. Thomas, J. E. Amonette, M. H. Engelhard,J. J. Antony, Y. Qiang, G. Duscher: Void formation during early stages of passivation: Initial oxidation of iron nanoparticles at room temperature, *J. Appl. Phys.* **2005**, *98*, 094308.

[46] U. Seip, M. -C. Tsai, K. Christmann, J. Küppers, G. Ertl: Interaction of Co with an Fe(111) Surface, *Surf. Sci.* **1984**, *139*, 29.

[47] A. Martínez-Arias, M. Fernández-Garíca, J. Soria, J. C. Conesa: Spectroscopic study of a Cu/CeO_2 catalyst subjected to redox treatments in carbon monoxide and oxygen, *J. Catal.* **1999**, *182*, 367.

[48] F. E. Wagner, S. Galvagno, C. Milone, A. M. Visco, L. Stievano, S. Calogero: Mössbauer characterisation of gold/iron oxide catalysts, *J. Chem. Soc., Faraday Trans.* **1997**, *93*, 3403.

[49] K. Liu, A. Q. Wang, W. S. Zhang, J. Wang, Y. Q. Huang, X. D. Wang, J. Y. Shen,T. Zhang: Microkinetic Study of CO Oxidation and PROX on Ir-Fe Catalyst, *Ind. Eng. Chem. Res.* **2011**, *50*, 758.

[50] J. Lin, B. T.Qiao, J. Y.Liu, Y. Q. Huang, A. Q. Wang, L. Li, W. S. Zhang, L. F. Allard, X. D. Wang, Design of a Highly Active $Ir/Fe(OH)_x$ Catalyst: Versatile Application of Pt-Group Metals for the Preferential Oxidation of Carbon Monoxide T. Zhang, *Angew. Chem. Int. Ed.* **2012**, *51*, 2920.

[51] J. L. Margitfalvi, I. Borbáth, K. Lázár, E. Tfirst, A. Szegedi, M. Hegedűs, S. Gőbölös: In situ characterization of $Sn-Pt/SiO_2$ catalysts used in low temperature oxidation of CO, *J. Catal.* **2001**, *203*, 94.